Journal of Computer Virology and Hacking Techniques (2019) 15:15–28
https://doi.org/10.1007/s11416-018-0323-0

ORIGINAL PAPER

Using convolutional neural networks for classification of malware represented as images

Daniel Gibert[1,2] · Carles Mateu[2] · Jordi Planes[2] · Ramon Vicens[1]

Received: 17 February 2018 / Accepted: 10 August 2018 / Published online: 27 August 2018

Abstract
The number of malicious files detected every year are counted by millions. One of the main reasons for these high volumes of different files is the fact that, in order to evade detection, malware authors add mutation. This means that malicious files belonging to the same family, with the same malicious behavior, are constantly modified or obfuscated using several techniques, in such a way that they look like different files. In order to be effective in analyzing and classifying such large amounts of files, we need to be able to categorize them into groups and identify their respective families on the basis of their behavior. In this paper, malicious software is visualized as gray scale images since its ability to capture minor changes while retaining the global structure helps to detect variations. Motivated by the visual similarity between malware samples of the same family, we propose a file agnostic deep learning approach for malware categorization to efficiently group malicious software into families based on a set of discriminant patterns extracted from their visualization as images. The suitability of our approach is evaluated against two benchmarks: the MalImg dataset and the Microsoft Malware Classification Challenge dataset. Experimental comparison demonstrates its superior performance with respect to state-of-the-art techniques.

Keywords Malware visualization · Malware classification · Convolutional neural network · Deep learning

1 Introduction

Malware, short for malicious software, refers to software programs designed to perform any kind of unwanted or harmful action on a computer system. This actions are targeted towards spying and stealing sensitive and critical information or damaging or modifying a compromised system. Nowadays, malware is a mature and growing business involving networks of developers and criminal organizations. It is a global industry worth millions of dollars that grows every year. According to McAfee [16] more than 600 million malicious programs were detected during the first quarter of 2017. However, the majority of new malware samples are deployed as variants of previously known samples. As a result, malicious software can be grouped together into families with each family originating from a single source base and exhibiting a set of consistent behaviors. In consequence, these shared characteristics between samples belonging to the same family might be used for detection and classification of unseen programs.

As the complexity and distribution of malware rises, the techniques used by malware developers to hide their malicious intent have improved. On the one hand, polymorphic malware uses a polymorphic engine to mutate the code while keeping the original functionality intact. Packing and encryption are the two most common ways to hide code. On the other hand, metamorphic malware rewrites its code every time it is propagated to an equivalent one. Traditionally, antivirus solutions relied on signature-based and heuristic-based methods. A signature is an algorithm or hash that uniquely identifies a specific malware. Given an unknown file, this method looks for any match between existing signatures in a database and the generated signature of the unknown file. Signatures are sensitive even to small program variations. On the contrary, heuristics are a set of rules determined by experts after

✉ Daniel Gibert
daniel.gibert@diei.udl.cat

Carles Mateu
carlesm@diei.udl.cat

Jordi Planes
jordi.planes@diei.udl.cat

Ramon Vicens
ramon.vicens@blueliv.com

[1] Blueliv, Leap in Value, Barcelona, Spain

[2] University of Lleida, Lleida, Spain

analyzing the behavior of malware. The main drawback of both approaches is that the malware has to be analyzed prior to the creation of these rules and heuristics. Unfortunately, such systems fail to predict new unseen malware and it is unfeasible to analyze manually every sample received. Thus, techniques to automatically categorize malware are required.

The main contributions of this paper are the following:

- The development of the first, to our knowledge, file agnostic deep learning system that learns visual features from executable files to classify malware into families. This is achieved by training a convolutional neural network on the representation of malware's binary content as gray scale images. Malware executables are visualized as gray scale images because its ability to capture minor changes while retaining the global structure is useful for detecting variations in samples.
- An extensive assessment of our technique using standard evaluation metrics (e.g. accuracy, precision, recall, F1-score) on two publicly available datasets, the MalIMG and the Microsoft Malware Classification Challenge datasets, one containing 9458 samples of 25 different malware families and a second containing 10868 samples of 9 different families, respectively.
- A comparative study of image-based machine learning techniques for malware classification. The experiments show that our model is capable of classifying samples from both datasets with 98.48% and 97.49% of accuracy, respectively, outperforming state-of-the-art methods in the literature.

The rest of the paper is organized as follows: Section 2 discusses the related research and describes the insights from representing malicious software as gray scale images. Section 3 introduces our deep learning approach for malware classification. Section 4 evaluates the performance of our method. Finally, Section 5 concludes with our remarks and future work suggestions.

2 Background

This section provides an overview of the types of analysis for determining the purpose and functionality of a given malware sample. Afterwards, it is provided a description of features and machine learning algorithms for addressing the problem of malware detection and classification.

2.1 Malware analysis

Malware analysis involves mainly two techniques: static analysis and dynamic analysis. Static analysis consists of examining the code or structure of a program without executing it. This kind of analysis can confirm whether a file is malicious, provide information about its functionality and can also be used to produce a simple set of signatures. The most common static analysis approaches are:

- Finding sequences of characters or strings. Searching through the strings of a program is the most simple way to obtain hints about its functionality. For instance, you can find strings related to printed messages, URLs accessed by the program, the location of files modified by the executable and names of common Windows dynamic link libraries (DLLs).
- Analysis of the Portable Executable File Format. The Portable Executable(PE) file format is used by Windows executables, object code and DLLs. Among the information it includes, the most useful pieces of information are the linked libraries and functions as well as the metadata about the file included in the headers.
- Searching for packed/encrypted code. Malware writers usually use packing and encryption to make their files more difficult to analyze. Software programs that have been packed or encrypted usually contain very few strings and higher entropy compared to legitimate programs.
- Disassembling the program, i.e. recovering the symbolic representation from the machine code instructions.

Dynamic analysis involves executing the program and monitoring its behavior on the system. Unlike static analysis, dynamic analysis allows to observe the actual actions executed by the a program. It is typically performed when static analysis has reached a dead end, either due to obfuscation and packing, or by having exhausted the available static analysis techniques. A survey on automated dynamic analysis techniques and tools is found in M. Egele et al [6]. Some techniques are:

- Function Call Monitoring. The behavior of the program is analyzed by using the traces containing the sequence of functions invoked by the executable under analysis.
- Function Parameter Analysis. Consists of tracking the values of parameters and function return values.
- Information Flow Tracking. Analyze how a program processes data and how data is propagated through the system.
- Instruction Trace. Analysis of the complete sequence of machine instructions executed by the program.

Both methods have its own advantages and disadvantages. On the one hand, static analysis is faster but suffers from code obfuscation, techniques used by malware authors to conceal the malicious purpose of the program. On the other hand, code obfuscation techniques and polymorphic malware fails at dynamic analysis because it analyses the runtime behavior

of a program by monitoring it while in execution. However, each malware sample must be executed in a safe environment for a specific time for monitoring its behavior, which is a very time consuming process. In addition, the environment might be quite different from the real runtime environment and malware may behave in different ways in the two environments, and under some conditions the actions of malware might not be triggered and thus, not logged.

2.2 Machine learning techniques for malware detection and classification

The use of machine learning algorithms to address the problem of malicious software detection and classification has increased during the last decade. The success of these approaches has increased thanks to: (1) the rise of commercial feeds of malware; (2) the reduction in cost of computing power; and (3) the advances made in the machine learning field. Several methods have been applied based on features extracted from both static and dynamic analysis. An overview is provided in Ranvee and Hiray [23] and Gandotra et al. [7]. Instead of directly dealing with raw malware, machine learning solutions first extract features that provide an abstract view of the software program. Then the features extracted are used to train a model. The type of features can be broadly divided into two groups: (1) static features and (2) dynamic features.

Static features are those extracted from the binary of the malware without executing it. One of the most common types of features is byte n-grams. An n-gram is a contiguous sequence of n items from a given sequence of text. In the work of Tesauro et al. [29] they extracted a list of byte-sequence trigrams and used an artificial neural network to classify malware. Similar to byte-sequence n-grams, approaches in the literature have used opcodes n-grams [4,25]. An opcode (abbreviated from operation code) is the portion of machine language instruction that specifies the operation to be performed. In particular, D. Yuxin et al. [32] used deep belief networks as a feature extractor to generate deep features to represent executables from their opcodes sequences. In addition, D. Gibert et al. [9] presented a convolutional neural network architecture to learn a set of discriminative subsequences from assembly language instructions. Features can also be extracted from the Portable Executable (PE) Header. The PE Header contains information about the files themselves such as the associated dynamically linked libraries and the sections of the program and their sizes. For instance, Ravi and Manoharan et al. [5] proposed a malware detection system based on Windows API call sequences. In addition, entropy has proven to be an effective feature to detect malware. The entropy of a program, refers to the amount of disorder (uncertainty) or its statistical variation. Entropy has commonly been used to detect encrypted and packed executables because these programs often have higher entropy. For example, in the dataset studied by Lydia et al. [17], native executables had an average entropy of 5.099 while packed and encrypted executables had an average entropy of 6.801, 7.175, respectively. Moreover, Bat-Erdene et al. [3] used entropy analysis to classify packing algorithms of given unknown packed executables.

Furthermore, dynamic features are those extracted by executing and observing the behavior of malware. Malware API calls have been used to model the behavior of malware. In [24], Z. Salehi et al. constructed dynamic features based on the name of API calls and each argument and return value recorded in a controlled environment during runtime. M. Ghiasi et al. [8] presented a framework for malware detection based on the changes in register contents. In [28], C.Storlie et al. presented a spine logistic regression model for malware detection, trained on the instruction traces extracted dynamically from computer programs. Additionally, B.Anderson [2] constructed graphs from the instruction traces of executables and applied graph kernels to create and compare similarity matrices of different computer programs.

Besides, several visualization techniques have been proposed in the literature to help malware analysis. Sorokin et al. [26] visualized a given executable using its structural entropy, obtained by dividing a binary into non-overlapping chunks and computing the entropy for each chunk. This representation was exploited by M. Wojnowicz et al. [31] and D. Gibert et al. [10] for detecting and categorizing malware, respectively. Lastly, Nataraj et al. [20] used image processing techniques to classify malicious software according to its visualization as gray scale images. In their work, they extracted GIST features from the malware images and trained a k-nearest neighbour for classification. The approach presented in this paper is motivated by the experiments of Nataraj et al. and in its visualization of the malware's binary content. Next, it is provided a detailed description of the visualization technique.

2.3 Visualizing malware as an image

To visualize a malware sample as an image, every byte has to be interpreted as one pixel in an image. Then, the resulting array has to be organized as a 2-D array and visualized as a gray scale image. Values are in the range [0,255] (0:black, 255:white).

Fig. 1 shows the representation of samples of malware belonging to nine different families as gray scale images. It can be observed that images of software executables from a given family are similar visually while distinct from those belonging to a different family. The main benefit of visualizing a malicious executable as an image is that the different sections of a binary can be easily differentiated. In addition, malware authors only used to change a small part of the code

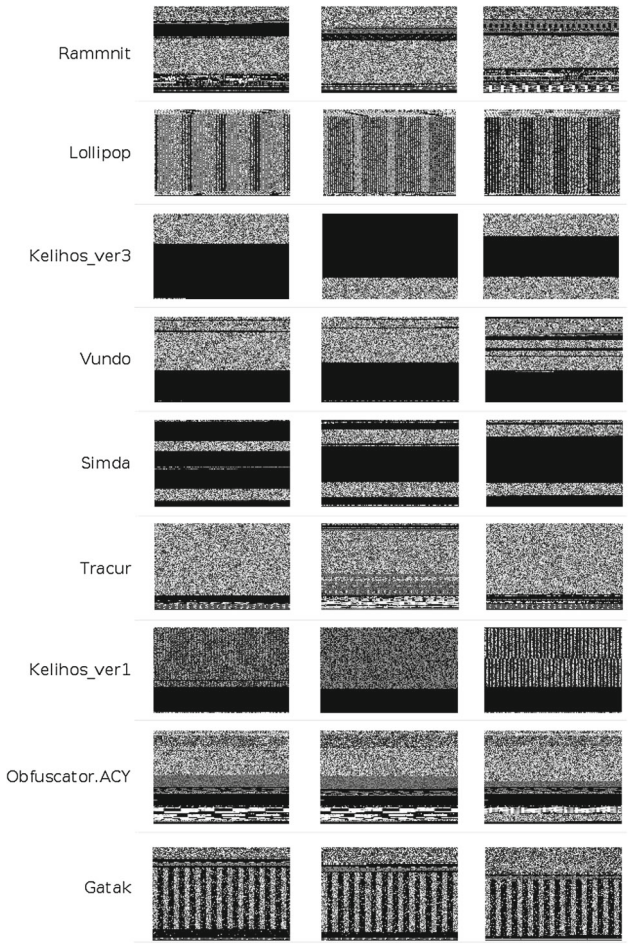

Fig. 1 Gray scale images of malicious software belonging to various families. Note that the images of malware belonging to the same family are similar while distinct from the images of malware from the rest of families

to produce new variants. Thus, if old malware is re-used to create new binaries the resulting ones would be very similar. Additionally, by representing malware as an image it is possible to detect the small changes while retaining the global structure of samples belonging to the same family.

In most cases, when observed in detail, one can notice several sections in the program, which usually have distinct feature patterns. Furthermore, the images stored in the resources section (.rsrc) of the PE file are also displayed (See Fig. 2). In addition, with this representation you can detect where zero-padding has been applied. Zero-padding is mainly used for block alignment but malware authors also use it to reduce the overall entropy of an executable.

2.4 Texture analysis and feature extraction

Traditional recognition approaches are composed of two stages: (1) feature extraction, transforming an observed signal into a robust representation, and (2) classification to

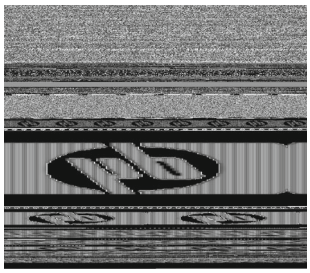

Fig. 2 Gray scale image representation of a malware sample containing a logo on their resources section

model decision-making. Consequently, their performance relies heavily on the discriminative power of the features extracted. Hand-engineered feature extractors [1,19,20] gather relevant information about an input and eliminate irrelevant variabilities. In summary, Nataraj et al. [20] and Narayanan et al. [19] extracted GIST and PCA features, respectively, and Ahmadi et al. [1] extracted both Haralick and local binary pattern features. Below is a brief description of the aforesaid methods.

GIST descriptors [22]. Given an image, the process to compute a GIST descriptor is as follows. First, the image is convolved with 32 Gabor filters with 8 orientations and 4 scales. Second, each feature map is divided into 16 regions of 4×4 values, and then the feature values are averaged within each region. Last, the 16 averaged values of all feature maps are concatenated.

PCA [12] features. Principal Component Analysis is a statistical procedure used for dimensionality reduction. It uses an orthogonal transformation to convert a set of observations of n possible correlated variables into a set of values with m linearly uncorrelated variables named principal components, where $n \leq m$.

Haralick [11] features have been used for image classification for years. The features are calculated by constructing a co-occurrence matrix, and computed by using the equations defined by Haralick such as the angular second-moment, contrast, correlation, etc.

Local binary pattern [21] features. The local binary pattern (LBP) feature of a given pixel is computed as follows. First, an 8 bit binary array is initialized as 0. Then, each pixel is compared with its neighboring pixels in clockwise direction. If the value of the neighboring pixel is greater or equal to 1 is assigned to its corresponding position. This gives an 8 bit binary array with zeros and ones. The 8-bit binary pattern is converted to a decimal number and is stored in the corresponding pixel location in the LBP mask. This process is applied to all pixels in an image. Once all LBP values have been calculated, the mask is normalized, resulting in 256 features.

3 Convolutional neural networks for malware classification

Convolutional neural networks (CNNs) [15] are a type of artificial neural network inspired by the mammals visual cortex [13], whose receptive field comprises sub-regions layered over each other to cover the entire visual field. This type of networks has long been used in visual recognition tasks such as image classification or object detection due to its ability to automatically extract discriminant and local features from images.

The core of a convolutional neural network consists of one or more convolutional layers and one or more fully connected layers. In particular, convolutional layers act as detection filters for the presence of specific features or patterns present in the data. The first layers detect lower level features whereas later layers detect increasingly high level features. On the contrary, fully connected layers are used at the end of a CNN to combine all the specific features detected by the previous layers and determine a specific target output. Figure 3 presents an overview of our CNN architecture. The hyper-parameters of the network had been selected using a grid search. The search was performed over the learning rate, the number of convolutional and fully-connected layers, and the size and number of kernels. The network architecture presented in this section correspond to the one that achieved better results during the evaluation.

The input of the network is an executable represented as a grayscale image $x^{w,h,d}$, where w and h are the width and the height of the image, respectively, and d is the depth ($d = 1$). Notice that in the work of Nataraj et al. [20] gray scale images had distinct widths and heights. This is because the size of each sample is different and with their preprocessing the width of the image was based on visual experiments and the height varied according to the file size. Thus, images had to be rescaled previously to feeding the convolutional neural network. The size of the resulting images has been adapted for every dataset during the experimentation in order to provide the best trade-off between accuracy and computational resources usage. Nevertheless, images have been resampled using the Lanzcos filter [30] as it provides the best compromise among several filters for multivariate interpolation.

The proposed neural network architecture has an input layer and three 4-stage feature extractors which learn hierarchical features through convolution, activation, pooling and normalization layers, as follows:

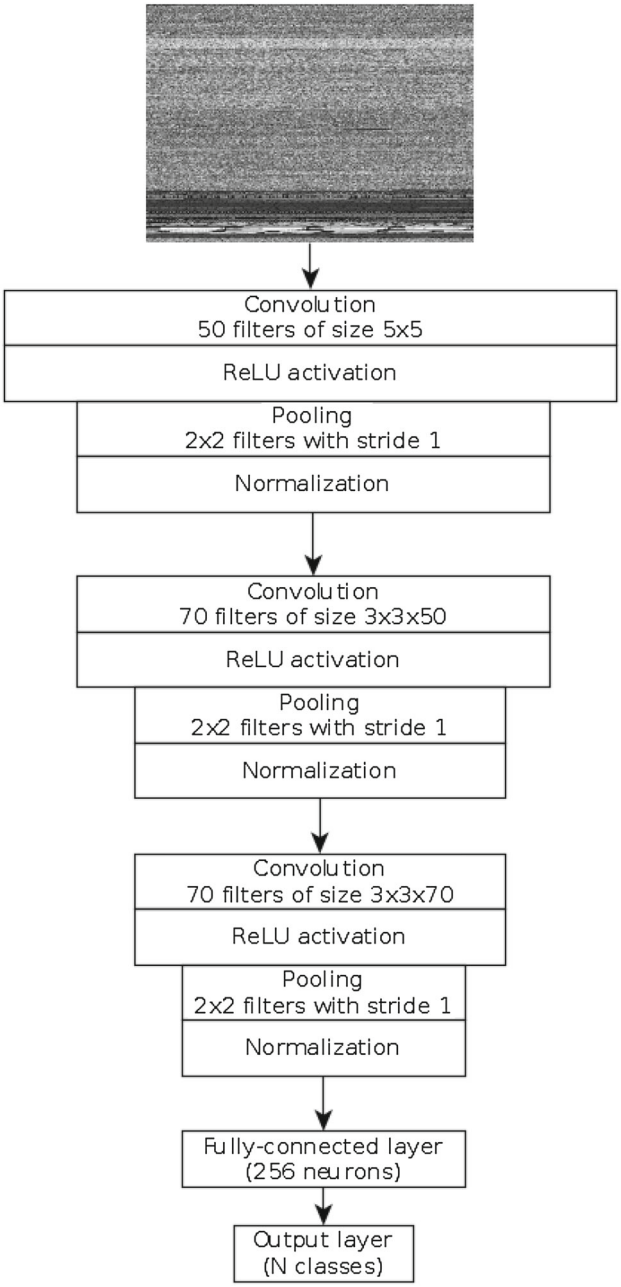

Fig. 3 Convolutional neural network for classification of malware represented as gray-scale images. It is composed by 3 convolutional layers followed by one fully-connected layer. The input of the network is a malicious program represented as a gray-scale image. The output of the network is the predicted class of the malware sample

> Convolution is an operation that takes an input signal of size $w \times h \times d$ and a filter of size $k \times k \times d$, where $k \leq w, h$, and produces one output signal. The kernel slides over each value of the input signal, multiplies the corresponding entries of the input signal and the kernel and adds them up. Figure 4 presents three of the filters learned in the first convolutional layer. It can be observed that the features these kernels detect are high changes in the pixels intensities. In particular, the convolutional layers are composed of 50, 70 and 70 filters of size $5 \times 5 \times 1$, $3 \times 3 \times 50$ and $3 \times 3 \times 70$ for the first, second and third convolutional layers, respectively.

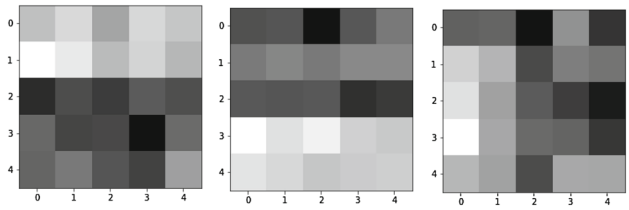

Fig. 4 Images of 3 filters randomly selected from the first convolutional layer

The activation function is used to signal distinct identification of likely features. Specifically, we used the ReLU [18] non-linear function, $y(x) = max(x, 0)$, in all activation layers.

The pooling operation reduces the spatial size of the features and provides some sort of robustness against noise and distortion. We applied max-pooling with filters of size $2 \times 2 \times 1$ with stride 1, which reduces the input signal by half, i.e. if the input signal's size is $128 \times 128 \times 1$, the output of applying max-pooling is an output signal of size $64 \times 64 \times 1$.

Normalization. The input values for different neurons in the layer are normalized using local response normalization [14] to inhibit and boost the neurons with relatively larger activations.

At the end of the extractor, the feature maps are flattened and combined to be used as input of the following fully-connected layer composed of 256 neurons. Afterwards, the output of the aforementioned layer is multiplied by the neurons of the output layer. Then, it is applied the softmax function to classify the binary program into its corresponding family. Notice that the number of neurons in the output layer depends on the number of families to classify: (i) the convolutional neural network trained to classify malware samples of the MalIMG dataset has 25 output neurons; (ii) the network trained to classify malicious software of the Microsoft Malware Classification Challenge dataset has 9 output neurons. In addition to normalization, to prevent overfitting we employed dropout [27], a regularization mechanism which randomly drops a proportion of p units during forward propagation and prevents the co-adaptation between neurons.

4 Evaluation

This section presents an empirical evaluation of the results obtained by our method in two datasets: the MalImg dataset [20], and the dataset provided by Microsoft for the Big Data Innovators Gathering Anti-Malware Prediction Challenge.

4.1 Experimental setup

The experiments were run on a single computer with the following hardware specifications:

- CPU: Intel i7-7700K
- Memory: 32 GB RAM
- GPU: Nvidia GTX 1080 Ti

To estimate the generalization performance of our approach we used K-fold cross validation. The dataset is divided into K equal size folds. Of the K subsamples, a single subsample is retained as the validation data for testing the model and the remaining subsamples are used as training data. This procedure is repeated as many times as there are folds, with each of the K folds used exactly once as the validation data.

Furthermore, to select the best model, additional evaluation metrics have been used: precision, recall and F1 score. This is because accuracy can be a misleading measure. Sometimes it may be desirable to select a model with a lower accuracy but with a greater predictive power on the problem (a.k.a. accuracy paradox). This occurs when there is as large class imbalance, where a model can predict the value of the majority class for all predictions and achieve a high classification accuracy while making mistakes on the minority or critical classes.

Precision (P) is the number of true positives (T_p) over the number of true positives plus the number of false positives (F_p).

$$P = \frac{T_p}{T_p + F_p}.$$

Recall (R) is the number of true positives (T_p) over the number of true positives plus the number of false negatives (F_n).

$$R = \frac{T_p}{T_p + F_n}.$$

The F1 score is the weighted average of precision, defined as following:

$$F_1 = 2 \cdot \frac{P \cdot R}{P + R}.$$

Since our target task is a multi-class classification problem, we used an adapted version of the F1 score named macro-averaged F1 score, defined as the average of the individual F1 scores obtained for each class.

$$macro\_F_1 = \frac{1}{q} \sum_{i=1}^{q} F_1^i$$

Table 1 MalImg: Distribution of Samples

Family	Class ID	#samples
Adialer.C	1	125
Agent.FYI	2	116
Allaple.A	3	2949
Allaple.L	4	1591
Allueron.gen!J	5	198
Autorun.K	6	106
C2Lop.P	7	146
C2Lop.gen!g	8	200
Dialplatform.B	9	177
Dontovo.A	10	162
Fakerean	11	381
Instantaccess	12	431
Lolyda.AA1	13	213
Lolyda.AA2	14	184
Lolyda.AA3	15	123
Lolyda.AT	16	159
Malex.gen!J	17	136
Obfuscator.AD	18	142
Rbot!gen	19	158
Skintrim.N	20	80
Swizzor.gen!E	21	128
Swizzor.gen!I	22	132
VB.AT	23	408
Wintrim.BX	24	97
Yuner.A	25	800

where q is the number of classes in the dataset and F_1^i is the F1 score of class i. Macroaveraging gives equal weight to each class. Thus, large classes will not dominate over small classes.

4.2 MalImg dataset

The MalImg dataset was provided by Nataraj et al. [20] and consists of 9342 gray scale images of 25 malware families. It contains samples of malicious software packed with UPX from different families such as Yuner.A, VB.AT, Malex.gen!J, Autorun.K and Rbot!gen. Additionally, there are images of family variants like the C2Lop.p and the C2Lop.gen!g or the Swizzor.gen!I and the Swizzor.gen!E. For more details, see Table 1.

4.2.1 Results

In order to train the network we downsampled the images to a fixed size. The width and height of the new images were set to 256. A lower value did not retain all the important information (i.e. lost discriminative information about a family) while higher values only increased the computational time without increasing the overall accuracy. For instance, if images were downsampled to 28×28 pixels, samples from the Yuner.A and the Autorun.K families became indistinguishable from one another and the model failed to classify correctly any sample belonging to the Autorun.K family. On the contrary, if images were downsampled to 128×128 pixels, the model classified correctly 42.45% of samples belonging to the Autorun.K family. Finally, if images are downsampled to 256×256 pixels, the percentage of correctly classified samples belonging to the Autorun.K family increased to 80.02%. In consequence, the macro-averaged F1 score increased from 0.948 to 0.958. See Tables 2 and 3 for more information.

The overall classification accuracy achieved by our method for the 25 malware families is higher than the approach of Nataraj et al., 0.9848 and 0.9718, respectively. As can be observed in Table 3, there were two major sources of misclassifications. On the one hand, the model classified incorrectly 21 samples of the Autorun.K family as belonging to the Yuner. That is because both families are compressed with UPX and their corresponding executables visualized as gray scale images only differ in the .rsrc section. As can be seen in Fig. 5, samples from the Autorun.K and Yuner.A families are indistinguishable to the human eye. On the other hand, the model had problems classifying samples belonging to variants of the same family, such as Swizzer.gen!E and Swizzer.gen!I. In particular, it only classified correctly 71% and 62% of their samples. If family variants are combined as one, the overall accuracy and F1 score is increased to 0.993 and 0.984, respectively. Specifically, the following families were grouped in one.

- Allaple.A and Allaple.L as Allaple.
- C2Lop.P and C2Lop.gen!g as C2Lop.
- Lolyda.AA1, Lolyda.AA2, Lolyda.AA3 and Lolyda.AT as Lolyda.
- Swizzor.gen!E and Swizzor.gen!I as Swizzor.

As observed in Table 4, by grouping the samples of family variants into a single family, the number of samples incorrectly classified was reduced. In particular, the samples misclassified belonging to variants of the Swizzor family was reduced from 87 to 26.

The main advantage of our approach with respect to the method of Ahmadi et al. [20] is two fold. First, our classification time is not penalized by the size of the training set, as it is the k-nearest neighbor algorithm; i.e. k-nn is a non-parametric, lazy learning algorithm and it does not learn a discriminative function from the training data but it "memorizes" the training data instead. In consequence, when a new file is received it goes through all training instances. Second, as GIST extracted features are based on

Table 2 MalIMG dataset confusion matrix for 10-fold cross validation using images of 128 × 128 pixels

Family	1	2	3	4	5	6	7	8	9	10	11	12	13	14	15	16	17	18	19	20	21	22	23	24	25	Precision	Recall	F1 Score
1	122	0	0	0	0	0	0	0	0	0	0	0	0	0	0	0	0	0	0	0	0	0	0	0	0	1.0	1.0	1.0
2	0	116	0	0	0	0	0	0	0	0	0	0	0	0	0	0	0	0	0	0	0	0	0	0	0	1.0	1.0	1.0
3	0	0	2949	0	0	0	0	0	0	0	0	0	0	0	0	0	0	0	0	0	0	0	0	0	0	1.0	0.99	0.99
4	0	0	0	1591	0	0	0	0	0	0	0	0	0	0	0	0	0	0	0	0	0	0	0	0	0	1.0	1.0	1.0
5	0	0	0	0	198	0	0	0	0	0	0	0	0	0	0	0	0	0	0	0	0	0	0	0	0	1.0	0.99	0.99
6	0	0	0	0	0	45	0	0	0	0	0	0	0	0	0	0	0	0	0	0	0	0	0	0	61	0.42	1.0	0.59
7	0	0	0	0	0	0	131	8	0	0	0	0	0	0	0	0	0	0	0	0	1	6	0	0	0	0.94	0.90	0.92
8	0	0	0	0	0	0	4	191	0	0	0	0	0	0	0	0	0	0	0	0	4	1	0	0	0	0.96	0.93	0.95
9	0	0	0	0	0	0	0	0	177	0	0	0	0	0	0	0	0	0	0	0	0	0	0	0	0	1.0	1.0	1.0
10	0	0	0	0	0	0	0	0	0	162	0	0	0	0	0	0	0	0	0	0	0	0	0	0	0	1.0	1.0	1.0
11	0	0	0	0	0	0	0	0	0	0	380	0	0	0	0	0	0	0	0	0	0	0	0	0	0	1.0	1.0	1.0
12	0	0	0	0	0	0	0	0	0	0	0	431	0	0	0	0	0	0	0	0	0	0	0	0	0	1.0	1.0	1.0
13	0	0	0	0	0	0	0	0	0	0	0	0	213	0	0	0	0	0	0	0	0	0	0	0	0	1.0	0.99	0.99
14	0	0	0	0	0	0	0	0	0	0	0	0	3	181	0	0	0	0	0	0	0	0	0	0	0	0.98	0.99	0.99
15	0	0	0	0	1	0	0	0	0	0	0	0	0	0	120	0	0	0	0	0	0	0	2	0	0	0.98	1.0	0.99
16	0	0	0	0	0	0	0	0	0	0	0	0	0	0	0	158	0	0	0	0	0	0	1	0	0	0.99	1.0	0.99
17	0	0	1	0	0	0	0	0	0	0	0	0	0	1	0	0	134	0	0	0	0	0	0	0	0	0.99	0.99	0.99
18	0	0	0	0	0	0	0	0	0	0	0	0	0	0	0	0	0	142	0	0	0	0	0	0	0	1.0	1.0	1.0
19	0	0	0	0	0	0	0	0	0	0	0	0	0	0	0	0	0	0	156	0	1	0	0	0	1	0.99	1.0	0.99
20	0	0	0	0	0	0	0	0	0	0	0	0	0	0	0	0	0	0	0	80	0	0	0	0	0	1.0	1.0	1.0
21	0	0	0	0	0	0	0	4	0	0	0	0	0	0	0	0	0	0	0	0	86	38	0	0	0	0.67	0.72	0.69
22	0	0	0	0	0	0	11	2	0	0	0	0	0	0	0	0	0	0	0	0	27	92	0	0	0	0.69	0.67	0.68
23	0	0	1	0	0	0	0	0	0	0	0	0	0	0	0	0	1	0	0	0	0	1	405	0	0	0.99	0.99	0.99
24	0	0	0	0	0	0	0	0	0	0	0	0	0	0	0	0	0	0	0	0	0	0	0	97	0	1.0	1.0	1.0
25	0	0	0	0	0	0	0	0	0	0	0	0	0	0	0	0	0	0	0	0	0	0	0	0	800	1.0	0.93	0.96
																										Macro-averaged F1 Score = 0,948		

Table 3 MalIMG dataset confusion matrix for 10-fold cross validation using images of 256 × 256 pixels

Family	1	2	3	4	5	6	7	8	9	10	11	12	13	14	15	16	17	18	19	20	21	22	23	24	25	Precision	Recall	F1 Score
1	122	0	0	0	0	0	0	0	0	0	0	0	0	0	0	0	0	0	0	0	0	0	0	0	0	1.0	1.0	1.0
2	0	116	0	0	0	0	0	0	0	0	0	0	0	0	0	0	0	0	0	0	0	0	0	0	0	1.0	1.0	1.0
3	0	0	2949	0	0	0	0	0	0	0	0	0	0	0	0	0	0	0	0	0	0	0	0	0	0	1.0	0.99	0.99
4	0	0	0	1591	0	0	0	0	0	0	0	0	0	0	0	0	0	0	0	0	0	0	0	0	0	1.0	1.0	1.0
5	0	0	0	0	198	0	0	0	0	0	0	0	0	0	0	0	0	0	0	0	0	0	0	0	0	1.0	0.99	0.99
6	0	0	0	0	0	85	0	0	0	0	0	0	0	0	0	0	0	0	0	0	0	0	0	0	21	0.80	1.0	0.89
7	0	0	0	0	0	0	138	6	0	0	0	0	0	0	0	0	0	0	0	0	1	1	0	0	0	0.95	0.87	0.88
8	0	0	0	0	0	0	5	192	0	0	0	0	0	0	0	0	0	0	0	0	2	0	0	0	0	0.96	0.94	0.95
9	0	0	0	0	0	0	0	0	177	0	0	0	0	0	0	0	0	0	0	0	0	0	0	0	0	1.0	1.0	1.0
10	0	0	0	0	0	0	0	0	0	162	0	0	0	0	0	0	0	0	0	0	0	0	0	0	0	1.0	1.0	1.0
11	0	0	3	0	0	0	1	0	0	0	376	0	0	0	0	0	0	0	0	0	1	0	0	0	0	0.99	1.0	0.99
12	0	0	0	0	0	0	0	0	0	0	0	431	0	0	0	0	0	0	0	0	0	0	0	0	0	1.0	1.0	1.0
13	0	0	0	0	0	0	0	0	0	0	0	0	213	0	0	0	0	0	0	0	0	0	0	0	0	1.0	0.99	0.99
14	0	0	0	0	0	0	0	0	0	0	0	0	3	181	0	0	0	0	0	0	0	0	0	0	0	0.98	0.99	0.98
15	0	0	0	0	1	0	0	0	0	0	0	0	0	0	121	0	0	0	0	0	0	0	1	0	0	0.98	1.0	0.99
16	0	0	0	0	0	0	0	0	0	0	0	0	0	1	0	157	0	0	0	0	0	0	0	0	0	0.99	1.0	0.99
17	0	0	1	0	0	0	0	0	0	0	0	0	0	1	0	0	134	0	0	0	0	0	0	0	0	0.99	0.99	0.99
18	0	0	0	0	0	0	0	0	0	0	0	0	0	0	0	0	0	142	0	0	0	0	0	0	0	1.0	1.0	1.0
19	0	0	0	0	0	0	0	0	0	0	0	0	0	0	0	0	0	0	157	0	1	0	0	0	0	0.99	1.0	0.99
20	0	0	0	0	0	0	0	0	0	0	0	0	0	0	0	0	0	0	0	80	0	0	0	0	0	1.0	1.0	1.0
21	0	0	0	0	0	0	1	5	0	0	0	0	0	0	0	0	0	0	0	0	91	31	0	0	0	0.71	0.71	0.71
22	0	0	0	0	0	0	14	2	0	0	0	0	0	0	0	0	0	0	0	0	32	82	1	0	1	0.62	0.71	0.66
23	0	0	0	0	0	0	0	0	0	0	0	0	0	0	0	0	1	0	0	0	0	1	406	0	0	0.99	0.99	0.99
24	0	0	0	0	0	0	0	0	0	0	0	0	0	0	0	0	0	0	0	0	0	0	0	97	0	1.0	1.0	1.0
25	0	0	0	0	0	0	0	0	0	0	0	0	0	0	0	0	0	0	0	0	0	0	0	0	800	1.0	0.97	0.98
																										Macro-averaged F1 Score = 0.958		

Table 4 MalIMG dataset confusion matrix for 10-fold cross validation using images of 256 × 256 pixels with family variants grouped into a single family. 1:Adialer.C; 2:Agent.FYI, 3:Allaple.A, Allaple.L; 4:Allueron.gen!J; 5:Autorun.K; 6:C2Lop.P, C2Lop.gen!g; 7:Dialplatform.B; 8:Dontovo.A; 9:Fakerean; 10:Instantaccess; 11:Lolyda,AA1; Lolyda.AA2; Lolyda.AA3, Lolyda.AT, 12:Malex.gen!J; 13:Obfuscator.AD; 14:Rbot!gen; 15:Skintrim.N; 16:Swizzor.gen!E, Swizzor.gen!I; 17:VB.AT; 18:Wintrim.BX; 19:Yuner.A

Family	1	2	3	4	5	6	7	8	9	10	11	12	13	14	15	16	17	18	19	Precision	Recall	F1 Score
1	122	0	0	0	0	0	0	0	0	0	0	0	0	0	0	0	0	0	0	1.0	1.0	1.0
2	0	116	0	0	0	0	0	0	0	0	0	0	0	0	0	0	0	0	0	1.0	0.99	0.99
3	0	0	4540	0	0	0	0	0	0	0	0	0	0	0	0	0	0	0	0	1.0	0.99	0.99
4	0	0	0	198	0	0	0	0	0	0	0	0	0	0	0	0	0	0	0	1.0	0.99	0.99
5	0	0	0	0	98	0	0	0	0	0	0	0	0	0	0	0	0	0	8	0, 92	1.0	0.96
6	0	0	0	0	0	330	0	0	0	0	0	0	0	0	0	0	16	0	0	0.95	0.92	0.93
7	0	0	0	0	0	0	177	0	0	0	0	0	0	0	0	0	0	0	0	1.0	1.0	1.0
8	0	0	0	0	0	0	0	162	0	0	0	0	0	0	0	0	0	0	0	1.0	0.99	0.99
9	0	0	1	0	0	2	0	0	377	0	0	0	0	0	0	0	1	0	0	0.99	1.0	0.99
10	0	0	0	0	0	0	0	0	0	431	0	0	0	0	0	0	0	0	0	1.0	1.0	1.0
11	0	1	0	1	0	0	0	1	0	0	676	0	0	0	0	0	0	0	0	0.99	0.99	0.99
12	0	0	2	0	0	0	0	0	0	0	1	133	0	0	0	0	0	0	0	0.98	0.99	0.98
13	0	0	0	0	0	0	0	0	0	0	0	0	142	0	0	0	0	0	0	1.0	1.0	1.0
14	0	0	0	0	0	0	0	0	0	0	0	0	0	158	0	0	0	0	0	1.0	1.0	1.0
15	0	0	0	0	0	0	0	0	0	0	0	0	0	0	80	0	0	0	0	1.0	1.0	1.0
16	0	0	0	0	0	25	0	0	0	0	0	0	0	0	0	234	1	0	0	0.90	0.99	0.94
17	0	0	0	0	0	0	0	0	0	0	0	1	0	0	0	2	405	0	0	0.99	0.96	0.97
18	0	0	0	0	0	0	0	0	0	0	0	0	0	0	0	0	0	97	0	1.0	1.0	1.0
19	0	0	0	0	0	0	0	0	0	0	0	0	0	0	0	0	0	0	800	1.0	0.99	0.99
																				Macro-averaged F1 Score = 0.984		

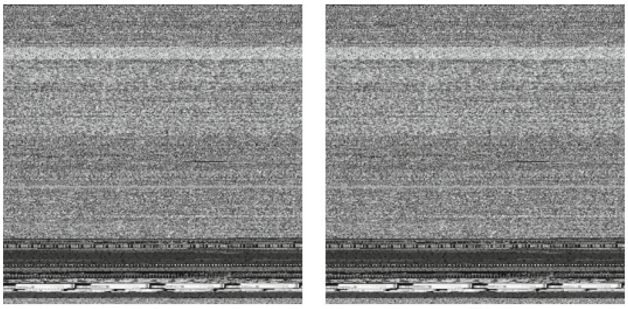

(a) (b)

Fig. 5 Autorun.K and Yuner.A samples downsampled to 256 × 256 pixels. The left image corresponds to the gray-scale visualization of a malware sample belonging to the Autorun.K family while the image in the right belongs to the Yuner.A family. Notice that both images are indistinguishable to the human eye

Table 5 BIG 2015: Distribution of Samples

Family	Class ID	#samples
Ramnit	1	1541
Lollipop	2	2478
Kelihos_ver3	3	2942
Vundo	4	475
Simda	5	42
Tracur	6	751
Kelihos_ver1	7	398
Obfuscator.ACY	8	1228
Gatak	9	1013

the global structure of an image if an adversary knows the technique it could avoid detection by reallocating different parts of the code. On the contrary, the changes produced by the code reallocation technique might not produce such undesired effects in our approach because convolutional networks are able to learn features invariant to translation, i.e. detect patterns which may be displaced in space, through the convolution and max-pooling operations. The convolution operation provides equivariance to translation. Afterwards, the max-pooling operation returns the largest value in its receptive field. In consequence, if the location of this value is still within the receptive field, the output of the pooling operation would not be altered. As a result, the combination of both operations together provide invariance to translation.

4.3 Microsoft malware classification challenge

Microsoft provided a dataset composed of 21741 samples for the Big Data Innovators Gathering (BIG 2015) Anti-Malware Prediction Challenge, 10868 for training and 10873 for testing. Every program in the dataset has a file containing the hexadecimal representation of the malware's binary content and its corresponding assembly file. However, only the label for the samples belonging to the training dataset is provided. Table 5 shows the distribution of malware programs present in the training dataset.

4.3.1 Results

Similar to the MalImg dataset, we downsampled the gray scale images. In particular, images from the BIG dataset were downsampled to 128 × 128 pixels because greater width and height did not improve the performance of the classifier. In addition, we performed 5-fold and 10-fold cross validation to evaluate our model. Tables 6 and 7 show the confusion matrices obtained for 5-fold cross validation and 10-fold cross validation.

Table 8 presents the results obtained by state-of-the-art approaches in the literature that had extracted image-based features to classify malware from the BIG dataset. To sum up, Narayanan et al. [19] used PCA to extract the first 10, 12 and 52 principal components and classify malware using different machine learning classification algorithms. Moreover, Ahmadi et al. [1] extracted Haralick and local binary pattern features from images and trained an ensemble of trees for classification. Their approaches were evaluated using 5-fold and 10-fold cross validation, respectively. As can be observed, our method outperformed the rest of approaches in

Table 6 BIG 2015 dataset confusion matrix for 5-fold validation using images of 128 × 128 pixels

Family	1	2	3	4	5	6	7	8	9	Accuracy
1	1492	7	0	2	2	11	3	19	5	0.968
2	6	2424	0	1	3	10	0	3	31	0.978
3	1	0	2937	0	0	0	4	0	0	0.998
4	2	1	2	461	2	2	1	2	2	0.971
5	3	3	0	4	25	1	0	6	0	0.595
6	10	5	1	3	1	701	1	18	11	0.933
7	2	0	1	0	0	0	392	0	3	0.985
8	36	4	1	13	2	19	5	1144	4	0.932
9	2	6	0	1	0	2	2	2	998	0.985

Table 7 BIG 2015 dataset confusion matrix for 10-fold validation using images of 128 × 128 pixels

Family	1	2	3	4	5	6	7	8	9	Accuracy
1	1490	4	2	2	2	9	1	28	3	0.967
2	6	2440	0	0	1	7	0	8	16	0.985
3	0	1	2938	1	0	0	2	0	0	0.999
4	3	0	2	461	2	1	1	3	2	0.971
5	3	2	0	1	29	2	0	5	0	0.690
6	8	6	1	2	0	713	2	10	9	0.948
7	1	0	5	1	0	0	391	0	0	0.982
8	44	4	2	8	2	17	5	1138	8	0.923
9	2	2	0	0	0	6	2	5	996	0.983

Table 8 Performance comparison of various methods for classification of BIG 2015 training dataset. 1-nearest neighbor (1-NN). Support vector machines (SVM). Static feed-forward network (SFN1 & SFN2). Dynamic feed-forward network (DFN)

Method	5-fold accuracy	Macro-averaged F1 Score
Haralick features + XGBoost	0.955	–
LBP features + XGBoost	0.951	–
CNN	0.973	0.927
	10-fold accuracy	
12 PCA features + 1-NN	0.966	0.910
10 PCA features + SVM	0.946	0.864
52 PCA features + SFN1	0.956	0.884
52 PCA features + SFN2	0.942	0.849
52 PCA features + DFN	0.955	0.889
CNN	0.975	0.940

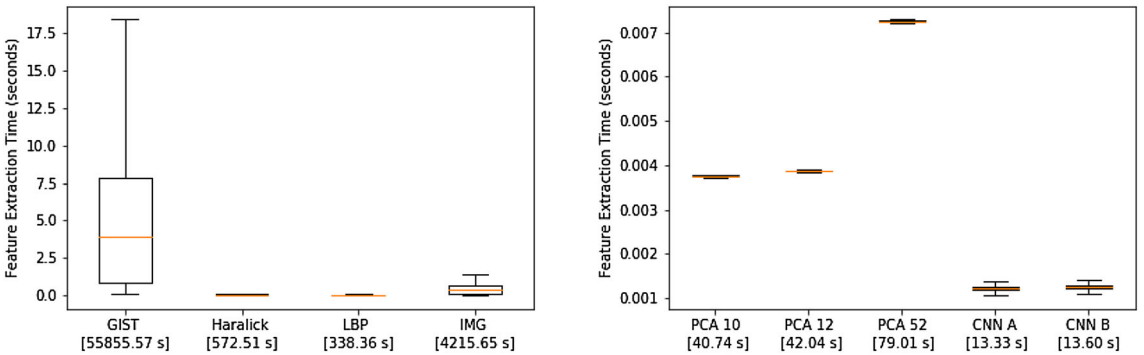

Fig. 6 The required time of feature extraction from the grayscale representation for each method. The time in brackets shows the total time of extraction for all training samples. LBP stands for local binary patterns. IMG denotes how much time it takes to transform a binary executable into a gray-scale image. PCA 10, PCA 12 and PCA 52 refer to the number of principal components used. CNN A refers to the time needed to extract the features by the convolutional network and CNN B refers to the time the networks needs to extract features and classify a sample

the literature, achieving 0.973 and 0.975 accuracy, for 5-fold and 10-fold cross validation, respectively. Furthermore, the average classification time of our approach is 0,001 seconds. Fig. 6 shows the computational time for every feature extraction method evaluated. The improvement of our method is equal to 99.98%, 98.47% and 96.06% with respect to the computational time needed to extract GIST, Haralick and local binary pattern features. Additionally, our method is 67.35%, 68.29% and 83.13% faster than the calculation of the 10, 12 and 52 principal components.

5 Conclusions

This paper presents a novel file agnostic deep learning system for classification of malware based on its visualization as gray-scale images. As far as we know, it is the first approach

to apply deep learning to find patterns from malware's binary content represented as images. The proposed solution has a number of advantages that allow malicious programs to be detected in a real-time environment. Firstly, it is file agnostic and is based solely on the binary code of an executable. Secondly, the transformation of an executable into a gray-scale image is inexpensive. Thirdly, the prediction time is lower than the rest of approaches. Fourthly, it obtained greater classification accuracy than all previous methods in the literature that were based on the representation of malware as gray-scale images.

5.1 Limitations and future work

Despite the fact that our approach was able to outperform state-of-the-art methods in terms of accuracy and classification time, it has some issues that are directly related to the visualization of malware as grayscale images. Even though it can be seen that the visualization of malware programs belonging to the same family has similar patterns, this approach has problems with some samples that have been compressed or encrypted, which may have a completely different overall structure. For instance, the visualization of samples from the Autorun.K and Yuner.A families are almost equal. To deal with such cases, we suggest combining the features extracted by the convolutional neural network with hand-designed features as input to a machine learning model based on distinct types of file features [1].

Acknowledgements We would like to thank the Blueliv Labs team, especially Daniel Solís, and Àngel Puigventós for their support and the feedback provided during the development of this work. This work has been partially funded by the Spanish MICINN Projects TIN2014-53234-C2-2-R, TIN2015-71799-C2-2-P and by AGAUR DI-2016-091.

Compliance with ethical standards

Conflict of interest The authors declare that they have no conflict of interest.

References

1. Ahmadi, M., Giacinto, G., Ulyanov, D., Semenov, S., Trofimov, M.: Novel feature extraction, selection and fusion for effective malware family classification. CoRR abs/1511.04317 (2015)
2. Anderson, B., Quist, D., Neil, J., Storlie, C., Lane, T.: Graph-based malware detection using dynamic analysis. J. Comput. Virol. **7**(4), 247–258 (2011). https://doi.org/10.1007/s11416-011-0152-x
3. Bat-Erdene, M., Park, H., Li, H., Lee, H., Choi, M.S.: Entropy analysis to classify unknown packing algorithms for malware detection. Int. J. Inf. Secur. **16**(3), 227–248 (2017)
4. Billar, D.: Opcodes as predictor for malware. Int. J. Electron. Secur. Digit. Forensics **1**, 156–168 (2007)
5. Chandrasekar Ravi, R.M.: Malware detection using windows API sequence and machine learning. Int. J. Comput. Appl. **43**, 12–16 (2012)
6. Egele, M., Scholte, T., Kirda, E., Kruegel, C.: A survey on automated dynamic malware-analysis techniques and tools. ACM Comput. Surv. **44**(2), 6:1–6:42 (2008). https://doi.org/10.1145/2089125.2089126
7. Gandotra, E., Bansal, D., Sofat, S.: Malware analysis and classification: a survey. J. Inf. Secur. **5**, 56–64 (2014)
8. Ghiasi, M., Sami, A., Salehi, Z.: Dynamic VSA: a framework for malware detection based on register contents. Eng. Appl. Artif. Intell. **44**, 111–122 (2015)
9. Gibert, D., Bejar, J., Mateu, C., Planes, J., Solis, D., Vicens, R.: Convolutional neural networks for classification of malware assembly code. In: International Conference of the Catalan Association for Artificial Intelligence, pp. 221–226 (2017). https://doi.org/10.3233/978-1-61499-806-8-221
10. Gibert, D., Mateu, C., Planes, J., Vicens, R.: Classification of malware by using structural entropy on convolutional neural networks. In: AAAI Conference on Artificial Intelligence (2018)
11. Haralick, R.M., Shanmugam, K., Dinstein, I.: Textural Features for Image Classification. IEEE Trans. Syst. Man Cybern. **SMC–3**(6), 610–621 (1973)
12. Hotelling, H.: Analysis of a complex of statistical variables into principal components. J. Educ. Psych. **24**, 417–441 (1933)
13. Hubel, D.H., Wiesel, T.N.: Receptive fields and functional architecture of monkey striate cortex. J. Physiol. (Lond.) **195**, 215–243 (1968)
14. Krizhevsky, A., Sutskever, I., Hinton, G.E.: Imagenet classification with deep convolutional neural networks. In: Proceedings of the 25th International Conference on Neural Information Processing Systems, NIPS'12, pp. 1097–1105. Curran Associates Inc., USA (2012)
15. Lecun, Y., Bottou, L., Bengio, Y., Haffner, P.: Gradient-based learning applied to document recognition. In: Proceedings of the IEEE, pp. 2278–2324 (1998)
16. LLC, M.: Mcafee labs threats report (2017). https://www.mcafee.com/us/resources/reports/rp-quarterly-threats-jun-2017.pdf. Accessed 20 Sept 2017
17. Lyda, R., Hamrock, J.: Using entropy analysis to find encrypted and packed malware. IEEE Secur. Anal. **5**, 40–45 (2007)
18. Nair, V., Hinton, G.E.: Rectified linear units improve restricted Boltzmann machines. In: Proceedings of the 27th International Conference on International Conference on Machine Learning, ICML'10, pp. 807–814. Omnipress, USA (2010)
19. Narayanan, B.N., Djaneye-Boundjou, O., Kebede, T.M.: Performance analysis of machine learning and pattern recognition algorithms for malware classification. In: Aerospace and Electronics Conference (NAECON) and Ohio Innovation Summit (OIS), 2016 IEEE National, pp. 338–342. IEEE (2016)
20. Nataraj, L., Karthikeyan, S., Jacob, G., Manjunath, B.S.: Malware images: visualization and automatic classification. In: Proceedings of the 8th International Symposium on Visualization for Cyber Security, VizSec '11, pp. 4:1–4:7. ACM, New York, NY, USA (2011)
21. Ojala, T., Pietikainen, M., Harwood, D.: Performance evaluation of texture measures with classification based on Kullback discrimination of distributions. In: Proceedings of the 12th IAPR International Conference on Pattern Recognition, 1994. Vol. 1—Conference A: Computer Vision amp; Image Processing, vol. 1 (1994)
22. Oliva, A., Torralba, A.: Modeling the shape of the scene: a holistic representation of the spatial envelope. Int. J. Comput. Vis. **42**(3), 145–175 (2001)
23. Ranvee, S., Hiray, S.: Comparative analysis of feature extraction methods of malware detection. Int. J. Comput. Appl. **120**, 1–7 (2015)

24. Salehi, Z., Sami, A., Ghiasi, M.: MAAR: robust features to detect malicious activity based on api calls, their arguments and return values. Eng. Appl. Artif. Intell. **59**, 93–102 (2017)
25. Shabtai, A., Moskovitch, R., Feher, C., Dolev, S., Elovici, Y.: Detecting unknown malicious code by applying classification techniques on OpCode patterns. Secur. Inf. **1**(1), 1 (2012). https://doi.org/10.1186/2190-8532-1-1
26. Sorokin, I.: Comparing files using structural entropy. J. Comput. Virol. **7**(4), 259 (2011)
27. Srivastava, N., Hinton, G., Krizhevsky, A., Sutskever, I., Salakhutdinov, R.: Dropout: a simple way to prevent neural networks from overfitting. J. Mach. Learn. Res. **15**, 1929–1958 (2014)
28. Storlie, C., Anderson, B., Vander Wiel, S., Quist, D., Hash, C., Brown, N.: Stochastic identification of malware with dynamic traces. Ann. Appl. Stat. **8**(1), 1–18 (2014). https://doi.org/10.1214/13-AOAS703
29. Tesauro, G., Kephart, J., Sorkin, G.B.: Neural networks for computer virus recognition. In: IEEE International Conference on Intelligence and Security Informatics, vol. 11 (1996)
30. Turkowski, K.: Filters for common resampling tasks. In: Glassner, A.S. (ed.) Graphics Gems, pp. 147–165. Academic Press Professional Inc., San Diego, CA (1990)
31. Wojnowicz, M., Chisholm, G., Wolff, M.: Suspiciously structured entropy: wavelet decomposition of software entropy reveals symptoms of malware in the energy spectrum. In: Florida Artificial Intelligence Research Society Conference (2016)
32. Yuxin, D., Siyi, Z.: Malware detection based on deep learning algorithm. Neural Comput. Appl. (2017). https://doi.org/10.1007/s00521-017-3077-6